Molecular determinant for run-down of L-type Ca^{2+} channels localized in the carboxyl terminus of the α_{1C} subunit

Klaus J. F. Kepplinger, Günter Förstner, Heike Kahr, Katharina Leitner, Patrick Pammer, Klaus Groschner†, Nikolai M. Soldatov* and Christoph Romanin

*Institute for Biophysics, University of Linz, A-4040 Linz, Austria, †Institute of Pharmacology and Toxicology, University of Graz, A-8010 Graz, Austria and *National Institute on Aging, NIH, Baltimore, MD 21224-6825, USA*

(Received 17 April 2000; accepted after revision 2 August 2000)

1. The role of the sequence 1572–1651 in the C-terminal tail of the α_{1C} subunit in run-down of Ca^{2+} channels was studied by comparing functional properties of the conventional $\alpha_{1C,77}$ channel with those of three isoforms carrying alterations in this motif.

2. The pore-forming α_{1C} subunits were co-expressed with $\alpha_2\delta$ and β_{2a} subunits in HEK-tsA201 cells, a subclone of the human embryonic kidney cell line, and studied by whole-cell and single-channel patch-clamp techniques.

3. Replacement of amino acids 1572–1651 in $\alpha_{1C,77}$ with 81 different amino acids leading to $\alpha_{1C,86}$ significantly altered run-down behaviour. Run-down of Ba^{2+} currents was rapid with $\alpha_{1C,77}$ channels, but was slow with $\alpha_{1C,86}$.

4. Transfer of the $\alpha_{1C,86}$ segments L (amino acids 1572–1598) or K (amino acids 1595–1652) into the $\alpha_{1C,77}$ channel yielded $\alpha_{1C,77L}$ and $\alpha_{1C,77K}$ channels, respectively, the run-down of which resembled more that of $\alpha_{1C,77}$. These results demonstrate that a large stretch of sequence between residues 1572 and 1652 of $\alpha_{1C,86}$ renders Ca^{2+} channels markedly resistant to run-down.

5. The protease inhibitor calpastatin added together with ATP was able to reverse the run-down of $\alpha_{1C,77}$ channels. Calpastatin expression was demonstrated in the HEK-tsA cells by Western blot analysis.

6. These results indicate a significant role of the C-terminal sequence 1572–1651 of the α_{1C} subunit in run-down of L-type Ca^{2+} channels and suggest this sequence as a target site for a modulatory effect by endogenous calpastatin.

The voltage-gated L-type Ca^{2+} channel is an essential part of signal transduction systems in many cell types triggering essential processes ranging from muscle contraction (Fabiato & Fabiato, 1979; Rios & Brum, 1987) to gene expression (Sheng *et al.* 1990; Murphy *et al.* 1991; Deisseroth *et al.* 1996, 1998). In electrophysiological studies usually carried out by the patch-clamp technique, activity of L-type Ca^{2+} channels decreases when the cytoplasmic side of the channels is perfused with an artificial intracellular solution. This phenomenon is called run-down and is most pronounced in cells dialysed internally in whole-cell recording or inside-out patches (Hagiwara & Byerly, 1983; Kostyuk, 1984; McDonald *et al.* 1994). So far, several mechanisms have been suggested for run-down, including proteolysis (Chad & Eckert, 1985; Belles *et al.* 1988*a*; Romanin *et al.* 1991) and dephosphorylation (Kostyuk, 1984; Armstrong & Eckert, 1987; Ono & Fozzard, 1992; Costantin *et al.* 1999). Alternatively, it has been suggested that wash-out of a cytoplasmic factor is the cause of run-down (M. Kameyama *et al.* 1988; A. Kameyama *et al.* 1997). Recent studies indicate that this factor might be calpastatin (Romanin *et al.* 1991; M. Kameyama *et al.* 1998), an endogenous inhibitor of the protease calpain (Molinari & Carafoli, 1998). The actions of calpastatin appear, however, not to be mediated through inhibition of calpain, as run-down is both reversible and not affected by synthetic calpain inhibitors (Seydl *et al.* 1995). Run-down has also been observed with Ca^{2+} channel subunits heterologously expressed in oocyte (Costantin *et al.* 1999) and mammalian expression systems (Höfer *et al.* 1997). The Ca^{2+} channel is a heteromeric protein complex that occurs in several subunit combinations (Hofmann *et al.* 1994; Catterall, 1995). It is composed of the pore-forming α_{1C} subunit and auxiliary β and $\alpha_2\delta$ subunits. The carboxyl terminus of the α_{1C} subunit has attracted much attention (Schultz *et al.* 1993; Soldatov *et al.* 1997, 1998) because of its potential involvement in channel gating. Removal of

Table 1. Structure of the variable parts in the carboxyl terminal tail of the α_{1C} subunits under investigation

$\alpha_{1C,77}$	IKTEGNLE**Q**ANEELRAIIKKIW**K**RTSM**K**LLDQVVPPAGDDEV**T**VGKFY**A**TFL-IQEYF**R**KFKKRKEQGLVGKPSQRNA**L**SL	(1572-1651)
$\alpha_{1C,77L}$	ETELSSQV**Q**YQAKEASLLERRR**K**SSHP	(1572-1598)
$\alpha_{1C,77K}$	SSHP**K**SSTKPNKLLSSGGS**T**GWVED**A**RAL**E**G**Q**VLAR**G**CGWLGSLEERERGPHHPP**L**GF	(1595-1652)
$\alpha_{1C,86}$	ETELSSQV**Q**YQAKEASLLERRR**K**SSHP**K**SSTKPNKLLSSGGS**T**GWVED**A**RAL**E**G**Q**VLAR**G**CGWLGSLEERERGPHHPP**L**GF	(1572-1652)

Amino acid sequences of $\alpha_{1C,77}$ (1572–1651) and $\alpha_{1C,86}$ (1572–1652) are shown in the top and bottom rows, respectively. Indicated amino acids of $\alpha_{1C,86}$ replace the respective residues in the amino acid sequence of $\alpha_{1C,77}$. In $\alpha_{1C,77L}$ and $\alpha_{1C,77K}$ subunits, indicated segments of $\alpha_{1C,86}$ replace the respective motifs L (1572–1598) and K (1595–1651) of the $\alpha_{1C,77}$ subunit. Note that the overlapping 4 amino acid segment SSHP has been proven not to contribute to the kinetics, voltage or Ca^{2+} dependence of inactivation (Soldatov *et al.* 1998). Residues in bold are located in identical positions between α_{1C} subunits.

approximately 70% of the tail causes an increase in the opening probability of the rabbit cardiac α_{1C} channel (Wei *et al.* 1994; Schmid *et al.* 1995) and accelerates inactivation of the human cardiac α_{1C} as compared to the wild-type channel (Klöckner *et al.* 1995). Besides the carboxyl tail several structural domains may contribute to channel inactivation properties (e.g. Speatgens & Zamponi, 1999). Alternative splicing of the human α_{1C} subunit generates multiple isoforms of the channel, including those with a structurally altered carboxyl terminal tail. Two human splice variants of the principal 2138 amino acid pore-forming α_{1C} subunit, a ubiquitous isoform $\alpha_{1C,77}$ and a hippocampal isoform $\alpha_{1C,86}$, show differences in their carboxyl terminal tail (Soldatov, 1992, 1994). Due to alternative splicing of exons 40–42, the $\alpha_{1C,77}$ channel has 80 amino acid residues (1572–1651) in the second quarter of the 662 amino acid carboxyl tail replaced with 81 non-identical amino acids yielding the $\alpha_{1C,86}$ splice variant (Table 1). These two channel splice variants, when expressed in *Xenopus* oocytes, exhibit strong differences in inactivation properties (Soldatov *et al.* 1997). Whole-cell Ba^{2+} currents of the $\alpha_{1C,86}$ channel inactivate significantly faster than those through $\alpha_{1C,77}$. Furthermore, with Ca^{2+} as charge carrier, inactivation of the current through $\alpha_{1C,77}$ is greatly accelerated in contrast to the $\alpha_{1C,86}$ inactivation rate, which is essentially Ca^{2+} independent (Soldatov *et al.* 1997). Furthermore, we have recently reported (Kepplinger *et al.* 2000) that the sequence 1572–1651 in the carboxyl terminus is also important for targeting, conductance and open probability. We additionally observed (N. M. Soldatov, unpublished observations) a difference in the reduction of Ba^{2+} currents over time between $\alpha_{1C,77}$ and $\alpha_{1C,86}$ channels in the oocyte expression system suggesting distinct run-down properties.

In an attempt to analyse the role of amino acids 1572–1651 in the regulation of Ca^{2+} channel run-down, we studied functional properties of the $\alpha_{1C,77}$ and $\alpha_{1C,86}$ channels and its two sub-segmental mutants, $\alpha_{1C,77K}$ and $\alpha_{1C,77L}$ (Table 1, Soldatov *et al.* 1998) in the HEK-tsA201 mammalian expression system. The results of our study indicate that the sequence 1572–1651 in the carboxyl terminal tail of the α_{1C} subunit determines not only channel inactivation but also run-down of L-type Ca^{2+} channels.

METHODS

Materials

Enhanced green fluorescent protein (EGFP) was purchased from Clontech (Heidelberg, Germany). The cDNA of the CD8 receptor (EBO pcD Leu2) was kindly provided by Richard Horn (Thomas Jefferson University Medical School, Philadelphia, PA, USA). Tissue culture media and reagents were purchased from Life Technology, Vienna, Austria. (−)BayK 8644 was from Research Biochemicals International, Vienna, Austria and all other chemicals from Sigma, Vienna, Austria. Magnetic beads carrying antibodies against the CD8 receptor were purchased from Dynal, Hamburg, Germany.

Molecular biology

Preparation of eukaryotic expression plasmids encoding $\alpha_{1C,77}$, $\alpha_{1C,86}$, $\alpha_{1C,77K}$ and $\alpha_{1C,77L}$ channels. All cDNAs of the human Ca^{2+} channel α_{1C} subunit used for eukaryotic transfection were prepared in the pcDNA3 vector (Invitrogen, Carlsbad, CA, USA). To incorporate Kozak sequence, the 5′-terminal RT-PCR clone 5′(2)6 (nucleotides (nt) −51–440) (Soldatov, 1992), obtained by the rapid amplification of cDNA ends (RACE) method, was subcloned into the Bluescript SK(−) vector (Stratagene, La Jolla, CA, USA) at *Hin*dIII, *Eco*RI sites, digested with *Hin*dIII and *Nco*I and ligated (160 ng) with a mixture of 18·2 pmol each of oligonucleotides 5′-AGCTTGGATCCGCCAC-3′ and 5′-CATGGTGGCGGATCCA-3′ which had been previously phosphorylated with T4 polynucleotide kinase (New England Biolabs, Beverly, MA, USA) in the presence of 10 mM ATP. Incorporation of the Kozak consensus sequence (5′-CCGCCA-3′) preceding the initiation codon was confirmed by sequence analysis. This construct was digested with *Hin*dIII at the 5′-flanking non-coding region and with *Mun*I (408) in an open reading frame (ORF), and the resulting 430 base pair fragment was ligated into the pHLCC77 at *Hin*dIII, *Mun*I sites to give pHLCC109. The 3′-terminal region was engineered using the cDNA hybrid (3275–6519) constructed in pBluescript SK(−) from the h2.05 cDNA (nt 3275–5267), which was supplemented at the 3′-end with a nucleotide sequence from the RT-PCR clone 3′t-12 (nt 5705–6519) obtained by the 3′-RACE extension of the ORF (Soldatov, 1992). This hybrid was cut at the 3′-UTR region with *Hpa*I (6515) and in the vector site with *Xba*I, the 3′-recessed ends were filled in using the Klenow fragment of DNA polymerase I (New England Biolabs) and ligated yielding pXIc. The 3′-terminal

*Sfu*I (3341), *Not*I fragment of pXIc was then ligated into pHLCC109 to replace the corresponding *Sfu*I/*Not*I fragment in pHLCC77B with modified 5′ and 3′ ends. Finally, the 5′ → 3′ *Hin*dIII, *Not*I cassette of pHLCC77B was subcloned into the pcDNA3 eukaryotic expression vector (Invitrogen). The integrity of the ORF was verified by sequencing.

86pcDNA3 was prepared by replacing the *Sfu*I (3341)/*Aat*II (5494) fragment of pHLCC77B with the corresponding fragment of pHLCC86 (Soldatov *et al.* 1997) and subcloning the *Hin*dIII, *Not*I cassette of the obtained pHLCC86B construct into the pcDNA3 vector. To prepare 77KpcDNA3 and 77LpcDNA3, the pHLCC77K and pHLCCL plasmids (Soldatov *et al.* 1998), respectively, were digested with *Bam*HI, blunt-ended using the Klenow DNA polymerase, digested with *Ppu*MI (2760) and the resulting 3′-terminal 3·9 kb fragments were ligated into 77pcDNA3 to replace the corresponding fragment in the *Ppu*MI (2760)/*Not*I (blunt-ended) cassette.

Nucleotide sequences of all PCR products, as well as ligation sites were verified using the ABI Prism dye terminator cycle sequencing kit with AmpliTaq DNA polymerase (Perkin-Elmer, Norwalk, USA).

Cell culture and transfection of HEK-tsA201 cells

HEK-tsA201 cells (kindly provided by Richard Horn, Thomas Jefferson University Medical School, Philadelphia, USA) were cultured in Dulbecco's modified Eagle's medium supplemented with streptomycin (100 μg ml^{-1}), penicillin (100 U ml^{-1}) and 10% fetal calf serum in a humidified atmosphere (95%) at 5% CO_2 and 37 °C. Cells were used for 12–14 passages and were transferred every 4 days. Transfection was performed using SuperFect (Qiagen, Hilden, Germany). In brief, cells exhibiting confluence of about 30–50% were transfected with 2·5 μg of total cDNA (molar ratio of α_{1C}:β_{2a}:$\alpha_2\delta$:EGFP:CD8 of 1:1·6:1·4:2·5:0·7). Transfection efficiency was estimated by counting cells showing EGFP fluorescence, and was in the range 20–60%. Furthermore, co-expression of the CD8 receptor and binding of CD8 antibody-coated beads (Dynal) was used as a visual marker to identify cells for electrophysiological experiments. Binding of the beads (range 3–15 per cell) was estimated to occur in 1–5% of the total number of cells.

Preparation of a supernatant of HEK-tsA201 cells

The HEK-tsA201 cell pellet obtained by centrifugation at 1000 *g* (10 min, 4 °C) was washed three times with PBS and finally resuspended in 0·4 M NaCl, 25% (v/v) glycerol, 1 mM EDTA, 0·5 mM DTT, protease inhibitors (×1000 of benzamidine, phenylmethylsulfonyl fluoride (PMSF), pepstatin) and 20 mM Hepes–Na (pH 7·9). Then the cells were lysed by freezing (liquid N_2, 1 min) and thawing (ice, 30 min). Cell debris and insoluble components were removed by centrifugation at 12 000 *g* (15 min, 4 °C) yielding the 12 000 *g* supernatant.

Immunoblot procedures

Western Blot was carried out according to Towbin *et al.* (1979) using a monoclonal antibody against human calpastatin (Takara Shuzo Co., Ltd, Japan; Clone CSL 1-5, Yokota *et al.* 1991). This antibody, which recognizes domain III of calpastatin, was generated in mouse, and its sensitivity is 10 pmol l^{-1} according to Yokota *et al.* 1991. Sigma calpastatin (55 μg) or the 12 000 *g* supernatant (100 μg) was separated by sodium dodecyl sulphate polyacrylamide gel electrophoresis (SDS-PAGE) on the gel and blotted onto a nitrocellulose membrane. Calpastatin from Sigma appears to be a crude preparation as observed in Coomassie Blue staining of the SDS gel. The membrane was then incubated with anti-calpastatin antibody, followed by incubation with peroxidase-conjugated rabbit anti-mouse IgG antibody (Sigma, Austria) and visualized using the Enhanced Chemiluminescence detection kit (Amersham, Austria). Control experiments have been carefully performed in the sole presence of the primary or secondary antibody and indicated clear specificity of the anti-calpastatin antibody.

Electrophysiology

Both whole-cell and single-channel patch-clamp recordings (Hamill *et al.* 1981) were obtained from successfully transfected HEK-tsA201 cells employing a List L/M EPC 7 amplifier.

Whole-cell recordings. The pipette solution contained (mM): caesium methane sulfonate 120, $CaCl_2$ 5, $MgCl_2$ 2, Hepes 10, EGTA 10, MgATP 2; pH (CsOH) 7·30. The bath solution consisted of (mM): *N*-methyl glucamine 154, $MgCl_2$ 1, D-glucose monohydrate 5, Hepes 10, 4-aminopyridine 5, $BaCl_2$ 15; pH (HCl) 7·40. Soft glass pipettes (microhaematocrit tubes, No. 564, Fa. Assistant, Vienna, Austria) with a resistance of 2–4 MΩ were used for whole-cell recordings. Ba^{2+} currents were activated by repetitive (0·2 Hz) depolarizations from a holding potential of −80 mV to test potentials (0·244 s) between −10 and +60 mV with an incremental increase of 5 or 10 mV. Current traces were filtered at 3 kHz, digitized at 8 kHz and were neither capacity nor leak current corrected in order to verify the quality of the voltage clamp. A liquid junction potential of 6 mV was determined but not taken into account. This value should be subtracted from all voltages in whole-cell recordings (Neher, 1992).

Single-channel recordings. Ba^{2+} currents through single Ca^{2+} channels were recorded in the cell-attached and inside-out configuration (Höfer *et al.* 1997). Cell potentials were set to approximately 0 mV by the use of a high K^+, low Cl^- extracellular solution that contained (mM): L-aspartic acid 110, KCl 20, $MgCl_2$ 2, Hepes 20, EGTA 2; pH (KOH) 7·35. The pipette solution consisted of (mM): $BaCl_2$ 96, Hepes 5; pH (NaOH) 7·40. The dihydropyridine Ca^{2+} channel activator (−)BayK 8644 (2·5 μM) was included in the pipette solution to facilitate channel activity in the cell-attached and inside-out configurations. Pipettes (GC150F-7.5F) were fabricated from borosilicate glass (Clark Medical Instruments, Pangbourne, UK) and had resistances of 4–6 MΩ. Sigmacote was used to reduce pipette capacitance. Single-channel currents of the channels were evoked by repetitive depolarizations (0·66 Hz) applied for 0·487 s from a holding potential of −80 mV to 0 mV ($\alpha_{1C,77}$) and 10 mV ($\alpha_{1C,86}$, $\alpha_{1C,77K}$ and $\alpha_{1C,77L}$). Single-channel traces were filtered at 1 kHz and digitized at 4 kHz. To recover channel activity from the usual run-down in inside-out patches, 2 mM Na_2ATP and 2 U ml^{-1} calpastatin (P-0787, Sigma, Munich, Germany) were added to the bath solution following patch excision. All experiments were performed at room temperature.

Analysis of electrophysiological data

Estimation of single Ca^{2+} channel activity was primarily based on the determination of the time course of mean channel activity NP_o (N is the total number of channels, P_o is the open probability; Schmid *et al.* 1995) determined for each depolarizing voltage pulse defined as a sweep. For this, single-channel sweeps are idealized using the 50% threshold method. The mean current I during one sweep of depolarization is determined and divided by the unitary current amplitude i to yield NP_o.

Statistics

Results are presented as means ± S.E.M. for the number of experiments usually given in parentheses. Student's two-tailed t test was used for statistical comparison considering differences statistically significant at $P < 0{\cdot}05$.

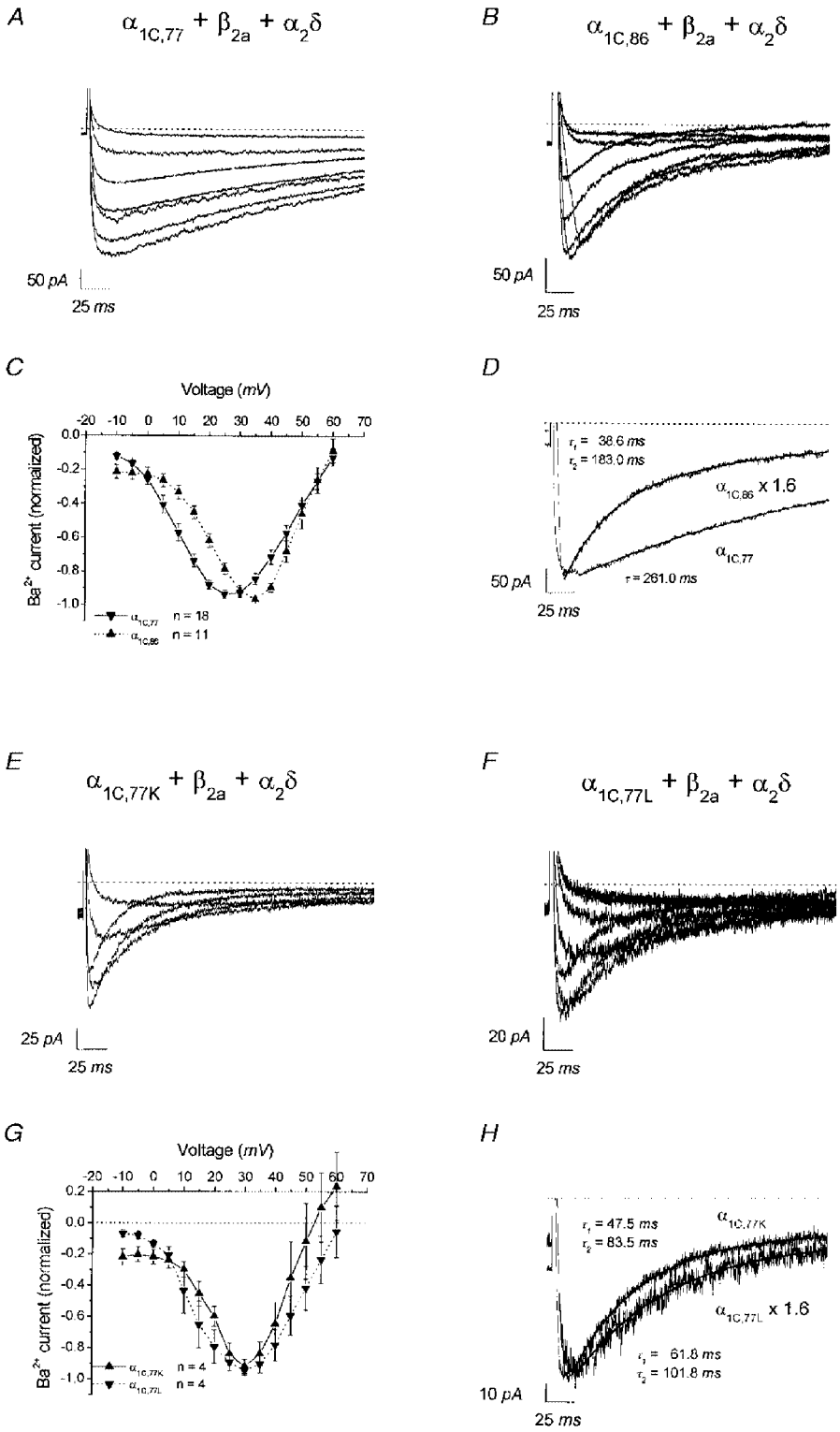

Figure 1. Whole-cell characteristics of the $\alpha_{1C,77}$, $\alpha_{1C,86}$, $\alpha_{1C,77K}$ and $\alpha_{1C,77L}$ channels

Representative whole-cell current traces with 15 mM Ba^{2+} as charge carrier obtained with $\alpha_{1C,77}$ (*A*), $\alpha_{1C,86}$ (*B*), $\alpha_{1C,77K}$ (*E*) and $\alpha_{1C,77L}$ (*F*) channels by repetitive (0·2 Hz) depolarizations from a holding potential of −80 mV to test potentials between −5 and 55 mV with an incremental increase of 10 mV. *C* and *G*, corresponding averaged current–voltage relationships derived from the indicated number of experiments, each normalized to maximum current. *D* and *H*, whole-cell traces recorded from $\alpha_{1C,77}$ and $\alpha_{1C,86}$ (*D*) as well as $\alpha_{1C,77K}$ and $\alpha_{1C,77L}$ channels (*H*) at a test potential of 25 mV were scaled with respect to the peak current size. Current decays were fitted by mono-exponential ($\alpha_{1C,77}$) and double-exponential ($\alpha_{1C,86}$, $\alpha_{1C,77K}$ and $\alpha_{1C,77L}$) functions yielding the indicated time constants. Dotted lines in *A* and *B*, and *D*–*H* denote zero current level.

RESULTS

Two human neuronal splice variants of α_{1C}, $\alpha_{1C,77}$ and $\alpha_{1C,86}$ (see Table 1), were transiently expressed together with β_{2a} and $\alpha_2\delta$ subunits in HEK-tsA201 cells. Electrophysiological characteristics of the whole-cell Ba^{2+} currents were initially determined, and the study was then extended to single-channel currents, which allowed for a further characterization of run-down, potentially determined by the carboxyl tail sequence 1572–1651. To narrow structures within this sequence, the two segmental mutants $\alpha_{1C,77L}$ and $\alpha_{1C,77K}$ were additionally studied in which segments of 27 (L) and 58 (K) amino acids, respectively, of $\alpha_{1C,86}$ replace the corresponding residues in the 80 amino acid sequence of $\alpha_{1C,77}$ (Table 1).

Whole-cell characteristics of the $\alpha_{1C,77}$, $\alpha_{1C,86}$, $\alpha_{1C,77K}$ and $\alpha_{1C,77L}$ channels

Figure 1 depicts an overview of whole-cell currents recorded with 15 mM Ba^{2+} as charge carrier. Representative current traces obtained by depolarizing voltage pulses between −5 and +55 mV for $\alpha_{1C,77}$, $\alpha_{1C,86}$, $\alpha_{1C,77K}$ and $\alpha_{1C,77L}$ are shown in Fig. 1*A*, *B*, *E* and *F*, respectively. Ba^{2+} currents through the $\alpha_{1C,77}$ channel exhibited a remarkably slower inactivation compared to those of the $\alpha_{1C,86}$, $\alpha_{1C,77K}$ and $\alpha_{1C,77L}$ channels. The corresponding current–voltage relationships (Fig. 1*C* and *G*) further revealed that the maximum of activation was shifted by ~10 mV to more positive values for $\alpha_{1C,86}$, $\alpha_{1C,77K}$ as well as $\alpha_{1C,77L}$ channels culminating at about 30–35 mV. Inactivation of Ba^{2+} currents (at 25 mV) through the $\alpha_{1C,77}$ channel was better fitted monoexponentially ($\tau = 412 \pm 64$ ms, $n = 8$), while that through $\alpha_{1C,86}$ exhibited a biexponential decay rate ($\tau_1 = 35 \pm 12$ ms; $\tau_2 = 216 \pm 72$, $n = 6$; Fig. 1*D*). Similar to $\alpha_{1C,86}$, both $\alpha_{1C,77K}$ and $\alpha_{1C,77L}$ channels exhibited rapid inactivation, where inactivation of both currents was best fitted by two exponentials ($\alpha_{1C,77K}$: $\tau_1 = 10 \pm 3$ ms, $\tau_2 = 60 \pm 10$ ms, $n = 5$; $\alpha_{1C,77L}$: $\tau_1 = 25 \pm 8$ ms, $\tau_2 = 113 \pm 32$ ms, $n = 4$; Fig. 1*H*) and

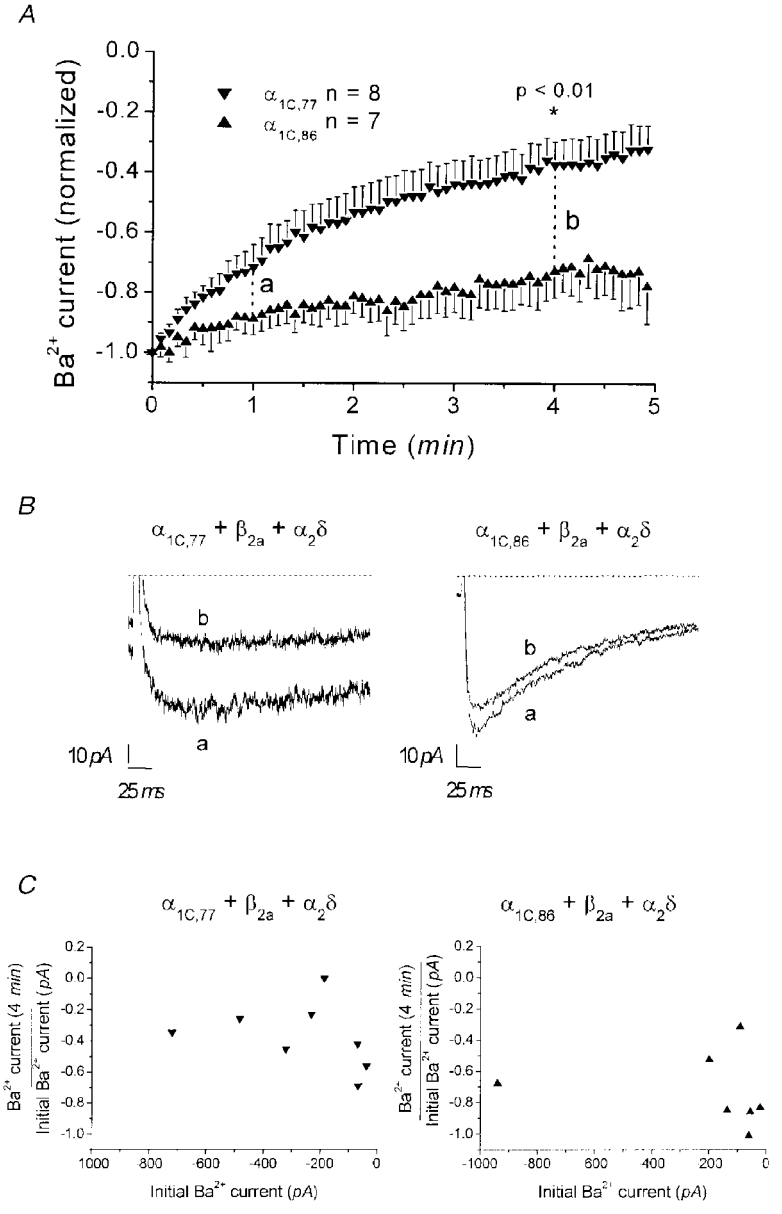

Figure 2. Time dependence of whole-cell Ba^{2+} currents through $\alpha_{1C,77}$ and $\alpha_{1C,86}$ channels

A, peak currents generated by repetitive depolarizations to 25 mV ($\alpha_{1C,77}$) and 35 mV ($\alpha_{1C,86}$). Comparison of currents at 4 min indicated a significant ($P < 0{\cdot}01$) difference in current size between the $\alpha_{1C,77}$ and $\alpha_{1C,86}$ channels. *B*, representative current traces recorded for $\alpha_{1C,77}$ and $\alpha_{1C,86}$ channels at 1 and 4 min as indicated in *A*. Dotted lines denote zero current level. *C*, the initial current (0 min) measured in each individual experiment for the respective channel is plotted against the normalized current reached after 4 min.

was slightly faster compared to that of the $\alpha_{1C,86}$ channel. These main differences between $\alpha_{1C,77}$ and $\alpha_{1C,86}$, $\alpha_{1C,77K}$ as well as $\alpha_{1C,77L}$ channels are consistent with those found in the oocyte expression system (Soldatov *et al.* 1997, 1998).

Run-down of whole-cell and single-channel currents of the $\alpha_{1C,77}$ and $\alpha_{1C,86}$ channels

In the course of whole-cell experiments, it appeared that the run-down behaviour of these channels was different (Fig. 2). The $\alpha_{1C,77}$ channel exhibited a remarkably faster run-down compared to the $\alpha_{1C,86}$ subunit. The peak current of $\alpha_{1C,77}$ declined to about $32 \pm 8\%$ ($n = 8$) within 5 min in contrast to $78 \pm 13\%$ ($n = 7$) that remained during the same time period with $\alpha_{1C,86}$ (Fig. 2*A*, $P < 0{\cdot}01$ at 4 min). Consistently, in double-electrode voltage-clamp experiments on oocytes the $\alpha_{1C,86}$ channel showed a $3 \pm 3\%$ ($n = 3$) decrease in I_{Ba} after 27–39 min compared to $27 \pm 10\%$ ($n = 4$) of the $\alpha_{1C,77}$ isoform after 22–38 min (N. M. Soldatov, unpublished observations). Run-down was characterized by a decrease of the peak current, whereas the rate of inactivation of whole-cell currents was not changed during run-down in either the $\alpha_{1C,77}$ or $\alpha_{1C,86}$ channel (Fig. 2*B*). Furthermore, the amount of run-down was not correlated with the size of the initial peak current for either channel (Fig. 2*C*), indicating that a smaller peak current did not necessarily correlate with a slower run-down.

The difference in run-down behaviour between the $\alpha_{1C,77}$ and $\alpha_{1C,86}$ channels was also visible in single-channel experiments following the formation of an inside-out patch (Fig. 3). Ca^{2+} channel activity (NP_o) of the $\alpha_{1C,77}$ channel decreased rapidly within 1 min (Fig. 3*A*). In contrast, the single-channel activity of $\alpha_{1C,86}$ remained largely unchanged for 3 min after patch excision and subsequently declined slowly (Fig. 3*B*). Corresponding single-channel traces for $\alpha_{1C,77}$ and $\alpha_{1C,86}$ are shown in Fig. 3*C* and *D*, respectively. The inset in Fig. 3*A* depicts the mean run-down behaviour of $\alpha_{1C,77}$ and $\alpha_{1C,86}$ channels yielding Ca^{2+} channel activities normalized to those of the cell-attached patch of $3{\cdot}1 \pm 0{\cdot}4\%$ ($n = 12$) and $65{\cdot}0 \pm 19{\cdot}1\%$ ($n = 6$), respectively, when

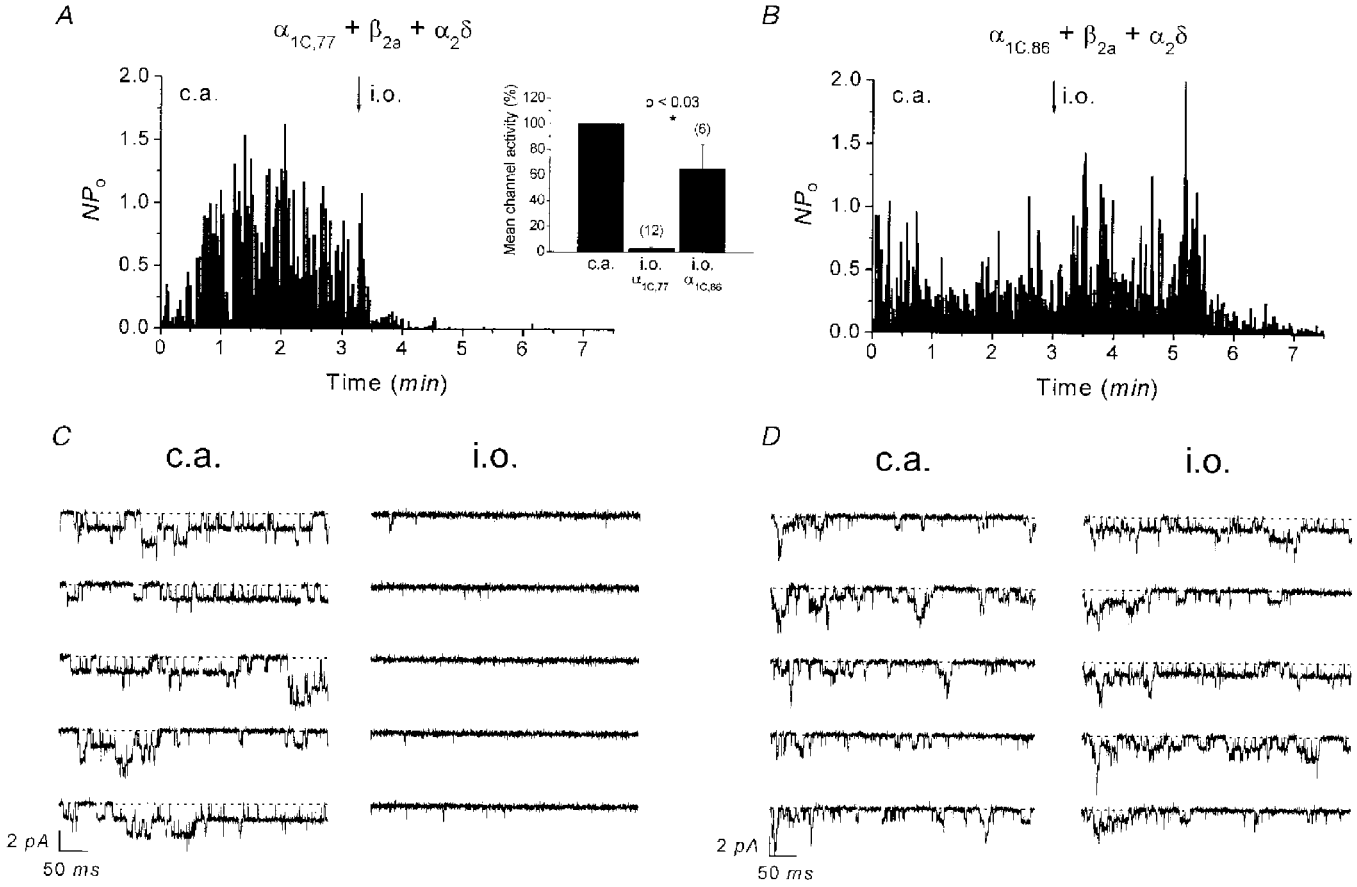

Figure 3. Time dependence of single-channel currents of $\alpha_{1C,77}$ and $\alpha_{1C,86}$ channels in cell-attached and inside-out patch configurations

Average channel activity (NP_o) of $\alpha_{1C,77}$ (*A*) and $\alpha_{1C,86}$ channels (*B*) recorded in the cell-attached (c.a.) patch followed by inside-out (i.o.) patch configuration. Inset in *A* shows mean channel activity reached 1·5–2·5 min after patch excision normalized to the previous activity in the cell-attached patch. Consecutive single-channel traces corresponding to the experiments in *A* and *B* are depicted in *C* and *D* both in the cell-attached and inside-out patch. Dotted lines indicate zero current level.

determined within 1·5–2·5 min after patch excision. Analysis of channel activity at a later time point (4·5–5·5 min) revealed 0% ($n = 12$) of $\alpha_{1C,77}$, whereas 6·1 ± 3·3% ($n = 5$) of $\alpha_{1C,86}$ activity was still left (not shown).

Run-down of whole-cell and single-channel currents of $\alpha_{1C,77L}$ and $\alpha_{1C,77K}$

To further pinpoint the molecular determinants for run-down within the sequence 1572–1651, we measured decline of the peak current over time in whole-cell recordings of $\alpha_{1C,77K}$ and $\alpha_{1C,77L}$ (Fig. 4*A*, see Table 1). Within 4 min in the whole-cell configuration, peak currents of both channels decreased to about half or even less of their initial value ($\alpha_{1C,77K}$: 53·2 ± 1·9%, $n = 5$; $\alpha_{1C,77L}$: 36·1 ± 16·8, $n = 3$) with no substantial change in their inactivation kinetics (Fig. 4*B*). Consistently, single Ca^{2+} channel activity of both $\alpha_{1C,77K}$ (Fig. 5*A*) and $\alpha_{1C,77L}$ (Fig. 5*B*) mutants exhibited a significant run-down following inside-out patch formation leading to a decrease in the mean channel activity to 23·0 ± 6·2% ($n = 6$) and 8·4 ± 4·7% ($n = 12$), respectively (Fig. 5*A*, inset), within 1·5–2·5 min after patch excision. At a later time point (4·5–5·5 min), almost no activity was visible for either $\alpha_{1C,77K}$ (0·6 ± 0·3%, $n = 6$) or $\alpha_{1C,77L}$ (0·7 ± 0·5%, $n = 6$) channels. Thus, these results indicate that the run-down behaviour of the $\alpha_{1C,77K}$ and $\alpha_{1C,77L}$ channels resembled more that of the $\alpha_{1C,77}$ channel in both whole-cell and single-channel experiments.

Effect of calpastatin on single Ca^{2+} channel activity of $\alpha_{1C,77}$, $\alpha_{1C,77L}$ and $\alpha_{1C,86}$ in the inside-out patch

Previous experiments have shown that run-down of L-type Ca^{2+} channels is reversed by the addition of calpastatin plus ATP to the intracellular face of the inside-out patch (Romanin *et al.* 1991; Seydl *et al.* 1995; A. Kameyama *et al.* 1998; M. Kameyama *et al.* 1998). Here we investigated the effect of calpastatin when applied to the $\alpha_{1C,77}$ and $\alpha_{1C,86}$ channels (Fig. 6). The complete run-down of the $\alpha_{1C,77}$ channel in the inside-out patch was largely reversed by addition of calpastatin plus ATP (Fig. 6*A*), excluding proteolysis as a mechanism of run-down. A qualitatively similar result was obtained with the $\alpha_{1C,77L}$ channel (data not shown). The $\alpha_{1C,86}$ channel showed, as demonstrated before, almost no run-down within 1·5 min following inside-out patch formation and the remaining channel activity was only slightly increased by calpastatin + ATP (Fig. 6*B*). Single-channel traces corresponding to $\alpha_{1C,77}$ and $\alpha_{1C,86}$ channel experiments are shown in Fig. 6*C* and *D*, respectively. Figure 6*E* illustrates that 56·7 ± 9·3% ($n = 9$) of the previously observed cell-attached $\alpha_{1C,77}$ channel activity recovered by the addition of calpastatin + ATP to the inside-out patch, while the activity of the $\alpha_{1C,86}$ channel reached 97·3 ± 14·0% ($n = 3$) under the same conditions.

To test whether calpastatin might be involved as an endogenous regulator of L-type Ca^{2+} channel activity in HEK-tsA201 cells, we examined its presence in these cells

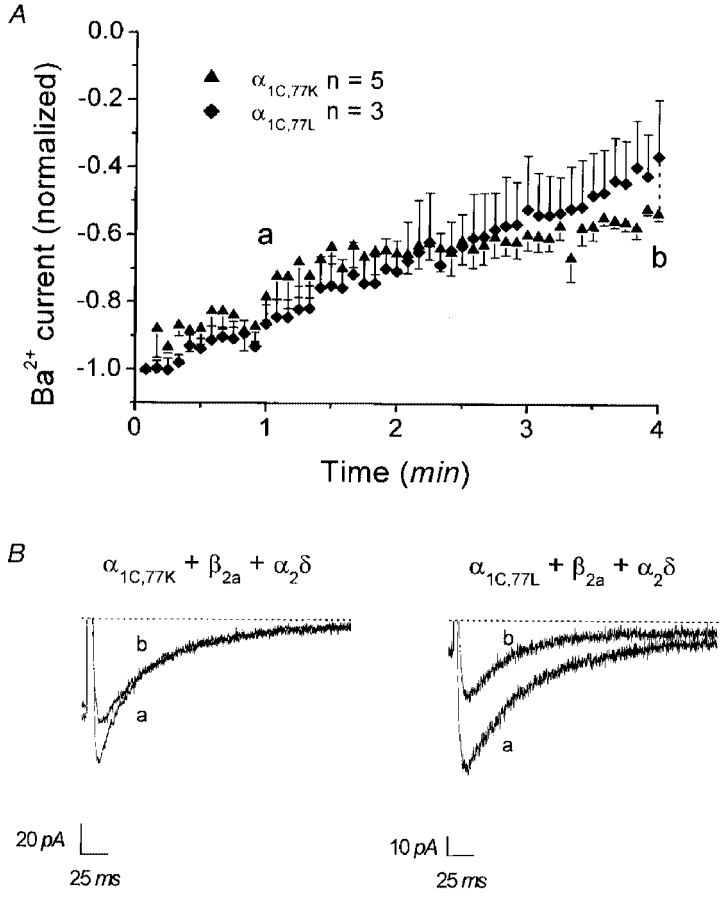

Figure 4. Time dependence of whole-cell currents of $\alpha_{1C,77K}$ and $\alpha_{1C,77L}$ channels

A, peak currents normalized to initial currents are shown as dependent on time for $\alpha_{1C,77K}$ and $\alpha_{1C,77L}$ channels recorded at test potentials of 35 mV. Comparison of currents at 4 min indicated no significant ($P > 0·05$) difference in current size between the $\alpha_{1C,77K}$ and $\alpha_{1C,77L}$ channels. *B*, representative current traces recorded for $\alpha_{1C,77K}$ and $\alpha_{1C,77L}$ channels at 1 and 4 min as indicated in *A*. Dotted lines denote zero current level.

using an anti-calpastatin antibody. Figure 6*F* presents immunoblots of Sigma rabbit skeletal muscle calpastatin used in the above experiments and of a 12 000 *g* supernatant prepared from HEK-tsA201 cells. Both lanes show the presence of specific bands indicative of calpastatin. Skeletal muscle calpastatin exhibited a relative molecular weight of 88 kDa. HEK-tsA201 calpastatin appeared at molecular sizes of 116, 84 and 64 kDa. The occurrence of calpastatin in various sizes from different tissues has been described (Molinari & Carafoli, 1997) as well as their efficacy in recovery of Ca^{2+} channels from run-down (M. Kameyama *et al.* 1998).

In summary, the run-down behaviour of the segmental mutants $\alpha_{1C,77K}$ and $\alpha_{1C,77L}$ resembled more that of the $\alpha_{1C,77}$ channel, whereas inactivation properties of these mutated channels were similar to that of the $\alpha_{1C,86}$ channel. Recovery from Ca^{2+} channel run-down was obtained with calpastatin, the natural occurrence of which was also confirmed in HEK-tsA201 cells.

DISCUSSION

In this study, we characterized the functional expression of the human L-type Ca^{2+} channel splice variants $\alpha_{1C,77}$ and $\alpha_{1C,86}$ as well as their segmental mutants $\alpha_{1C,77K}$ and $\alpha_{1C,77L}$ in the mammalian cell line HEK-tsA201. Our results strongly suggest that the sequence 1572–1651 in the carboxyl terminal tail of α_{1C} is important for the run-down phenomenon of L-type Ca^{2+} channels.

Electrophysiological features of α_{1C} splice variants and segmental mutants in whole-cell and single-channel experiments

The $\alpha_{1C,77}$ channel exhibited a significantly slower inactivation than $\alpha_{1C,86}$ and the two segmental mutants $\alpha_{1C,77K}$ and $\alpha_{1C,77L}$ in both whole-cell and single-channel experiments. These data substantiated the role of the sequence 1572–1651 and of its L and K segments (see Table 1) as molecular determinants of voltage-dependent inactivation (Soldatov *et al.* 1998).

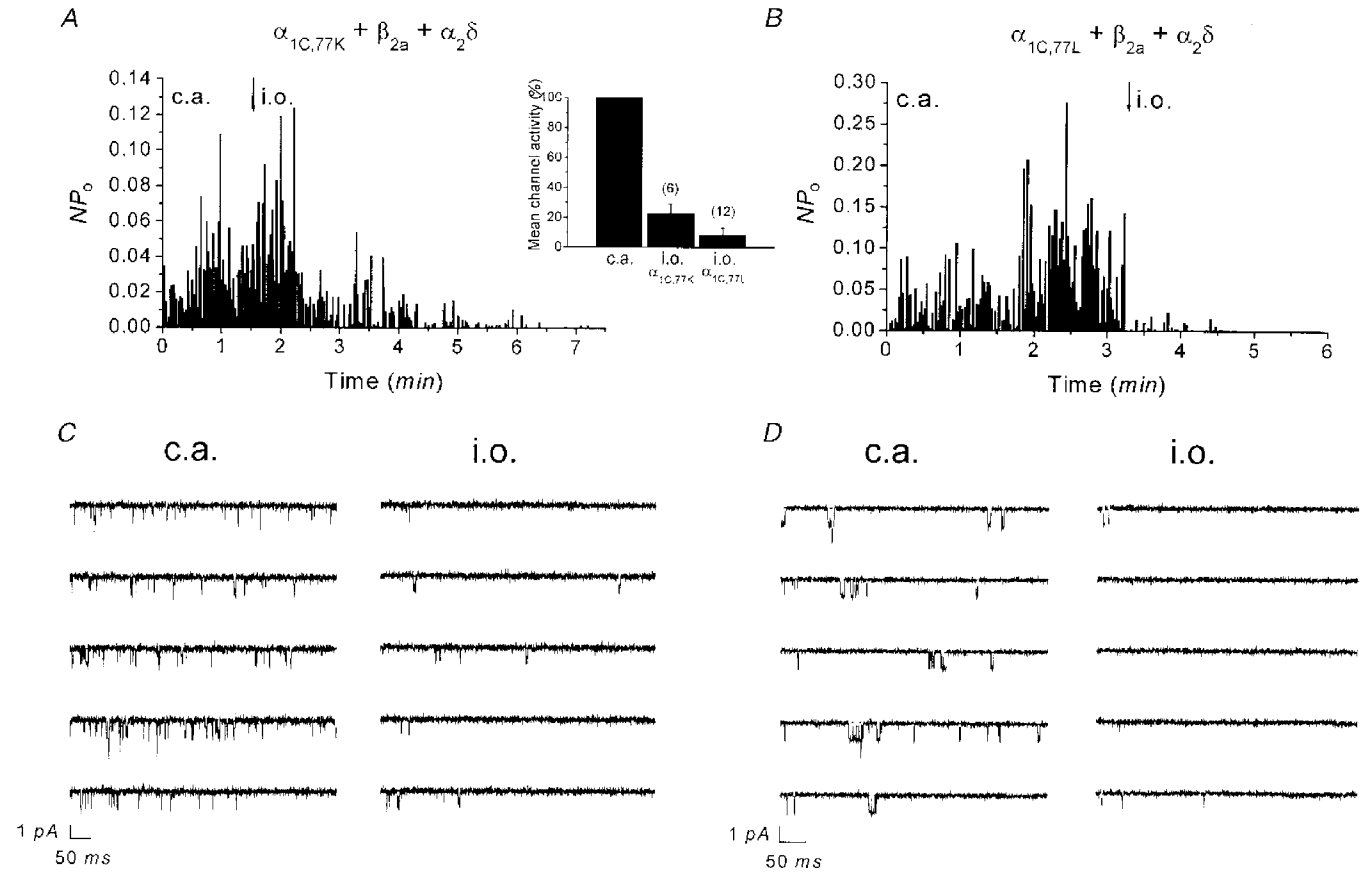

Figure 5. Time dependence of single-channel Ba^{2+} currents through $\alpha_{1C,77K}$ and $\alpha_{1C,77L}$ channels in cell-attached and inside-out patch configurations

Average channel activity (NP_o) of $\alpha_{1C,77K}$ (*A*) and $\alpha_{1C,77L}$ (*B*) channels recorded in the cell-attached (c.a.) patch followed by inside-out (i.o.) patch configuration. Inset in *A* shows mean channel activity reached 1·5–2·5 min after patch excision normalized to the preceding activity in the cell-attached patch. Consecutive single-channel traces corresponding to the experiments in *A* and *B* are depicted in *C* and *D* both in the cell-attached and inside-out patch. Single channel openings are visible as downward deflections.

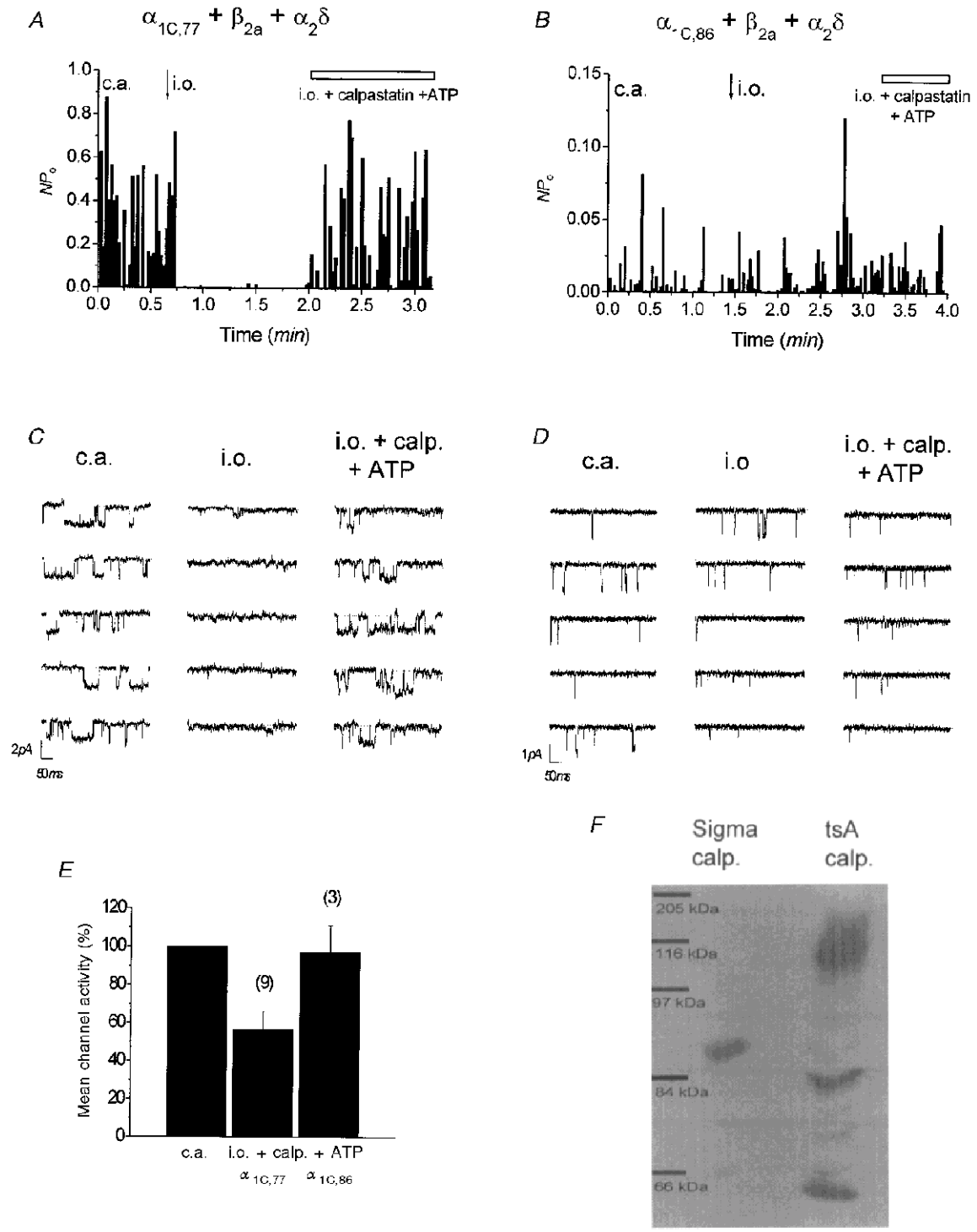

Figure 6. Effect of calpastatin + ATP on the activity of single $\alpha_{1C,77}$ and $\alpha_{1C,86}$ channels in the inside-out patch

Time course of average channel activity (NP_o) of $\alpha_{1C,77}$ (*A*) and $\alpha_{1C,86}$ (*B*) in the cell-attached (c.a.) and inside-out (i.o.) patch before and after addition of calpastatin (2 U ml^{-1}) + Na_2ATP (1 mM). Single-channel activity of $\alpha_{1C,77}$ almost completely recovered from run-down in the inside-out (i.o.) patch, whereas almost no effect was observed on channel activity of $\alpha_{1C,86}$, which was resistant to run-down in the i.o. patch. *C* and *D* depict single-channel traces for the corresponding experiments in *A* and *B*, recorded under the indicated conditions. Single channel openings are visible as downward deflections. *E*, mean channel activity of $\alpha_{1C,77}$ and $\alpha_{1C,86}$ in the presence of calpastatin + ATP, normalized to the preceding channel activity in the cell-attached configuration. *F*, representative Western blot analysis ($n = 4$) of Sigma calpastatin and HEK-tsA201 cell 12 000 *g* supernatant using an anti-calpastatin antibody.

Molecular determinants of run-down

Conventional L-type Ca^{2+} channels are subject to run-down in both whole-cell (Belles *et al.* 1988*b*) and inside-out configurations (Cavalie *et al.* 1983; Romanin *et al.* 1991). However, L-type Ca^{2+} channels have been found in hippocampal neurones (Kavalali & Plummer, 1997), which show almost no run-down under cell-free conditions. Similarly, anomalous L-type channels in motoneurones are resistant to run-down (Hivert *et al.* 1999). Run-down has been reported to occur on the α_{1C} subunit (Hao *et al.* 1998; Costantin *et al.* 1999) suggesting that the site of regulation that is the cause of run-down is located on the pore-forming subunit itself. In accordance, the results presented here imply that the sequence 1572–1651 in the carboxyl terminal tail of the α_{1C} subunit is one molecular determinant of run-down. The whole-cell experiments performed revealed an essentially slower run-down of the $\alpha_{1C,86}$ channel compared to the conventional $\alpha_{1C,77}$. As peak currents of $\alpha_{1C,86}$ were usually smaller than those observed with $\alpha_{1C,77}$, a faster run-down might be correlated with larger currents independent of the structural difference between $\alpha_{1C,77}$ and $\alpha_{1C,86}$. However, no correlation was found between the current size and the amount of run-down for $\alpha_{1C,77}$ and $\alpha_{1C,86}$ channels. Consistently, $\alpha_{1C,77}$ and $\alpha_{1C,86}$ channels exhibited a significantly different run-down in oocytes. The whole-cell data were substantiated by single-channel experiments in which I_{Ba} through $\alpha_{1C,86}$ showed a significantly slowed run-down within 1·5–2·5 min following patch excision, in contrast to a rapid run-down of $\alpha_{1C,77}$ within the same time period. As run-down was not completely abolished, other structures within the α_{1C} subunit might additionally contribute to this process. The qualitatively similar results obtained in whole-cell and single-channel configurations indicated that the presence of the Ca^{2+} agonist (–)BayK 8644 in single-channel experiments exerted no main effect on run-down behaviour. In both whole-cell and single-channel experiments the segmental mutants $\alpha_{1C,77K}$ and $\alpha_{1C,77L}$ showed a similar and substantial run-down which resembled more that of the $\alpha_{1C,77}$ channel, indicating that a large stretch of the 81 amino acid sequence of the $\alpha_{1C,86}$ subunit is required to markedly reduce run-down of L-type Ca^{2+} channels. As this sequence also determines channel inactivation (Soldatov *et al.* 1997, 1998), both channel properties may be interdependent. However, the segmental mutants in contrast to the $\alpha_{1C,86}$ channel displayed a fast run-down, though they all showed rapid Ba^{2+} current inactivation. In addition, the inactivation rate did not change during run-down. Thus, the mechanism of run-down seems to be different from that governing channel inactivation.

Mechanism of run-down

Dephosphorylation and wash-out of a regulatory factor have been suggested as prime mechanisms responsible for channel run-down. Reversal of run-down by protein kinase A (PKA) is controversial. While Ono & Fozzard (1992) reported a clear recovery from run-down, Costantin *et al.* (1999) observed an effect only in a subset of patches and Yazawa *et al.* (1997) found a recovery of channel activity essentially independent of PKA. The functionally important PKA phosphorylation site (De Jongh *et al.* 1996; Gao *et al.* 1997) is not present within the sequence 1572–1651 in the $\alpha_{1C,77}$ channel, whereas a putative motif (R/KRXS) is found in the $\alpha_{1C,86}$ channel within the L segment (amino acids 1592–1595). However, a role of this putative PKA site in the sensitivity of Ca^{2+} channels to run-down is rather unlikely as the $\alpha_{1C,77L}$ contains this motif and showed a rapid run-down similar to the $\alpha_{1C,77}$ channel.

Wash-out of a regulatory factor has been suggested as the second mechanism of run-down. It has been reported that the ubiquitous protein calpastatin is an important cytoplasmic factor regulating L-type Ca^{2+} channel activity (Romanin *et al.* 1991; Seydl *et al.* 1995; M. Kameyama *et al.* 1998; Hao *et al.* 1999). Calpastatin has been also detected in oocytes (Lorca *et al.* 1991), and as shown here in HEK-tsA201 cells, where overexpression of calpastatin was found to increase L-type Ca^{2+} channel activity (K. Leitner & C. Romanin, unpublished observations). Indeed, the activity of the $\alpha_{1C,77}$ channel subjected to run-down following inside-out patch formation was recovered by addition of calpastatin + ATP to the intracellular face of the membrane. Disturbances of the calpain–calpastatin system have been claimed to be related to a number of pathological conditions such as cardiac ischaemia, stroke and brain trauma (Molinari & Carafoli, 1997), suggesting a physiological role of endogenous calpastatin in the regulation of Ca^{2+} channel activity.

Run-down has been reported to occur without changes in the gating currents (Josephson & Varadi, 1996; Costantin *et al.* 1999) suggesting a disruption of the linkage between the voltage sensor and the opening of the ionic gate (Costantin *et al.* 1999). Thus it is tempting to speculate that the sequence 1572–1651 that determines run-down properties represents the target site for the modulatory effects of calpastatin + ATP, which then restore coupling of the ionic gate to the voltage sensor, resulting in channel opening upon depolarization. A calmodulin-binding IQ region (1624–1635) within the sequence 1572–1651 has been recently reported as a critical site for Ca^{2+}-induced inactivation (Peterson *et al.* 1999; Qin *et al.* 1999; Zühlke *et al.* 1999). Hence, a cross-talk between Ca^{2+} channel regulation by calpastatin + ATP and Ca^{2+} appears possible and remains to be investigated in future studies.

In summary, the amino acid sequence 1572–1651 in the carboxyl terminal tail of the α_{1C} subunit is critical for channel inactivation, and independently represents an important structure for L-type Ca^{2+} channel run-down.

Armstrong, D. L. & Eckert, R. (1987). Voltage-dependent Ca^{2+} channels that must be phosphorylated to respond to membrane depolarization. *Proceedings of the National Academy of Sciences of the USA* **84**, 2518–2522.

Belles, B., Hescheler, J., Trautwein, W., Blomgren, K. & Karlsson, J. O. (1988*a*). A possible physiological role of the Ca-dependent protease calpain and its inhibitor calpastatin on the Ca^{2+} current in guinea pig myocytes. *Pflügers Archiv* **412**, 554–556.

Belles, B., Malecot, C. O., Hescheler, J. & Trautwein, W. (1988*b*). 'Run-down' of the Ca current during whole-cell recordings in guinea pig heart cells: role of phosporylation and intracellular Ca^{2+}. *Pflügers Archiv* **411**, 353–360.

Catterall, W. A. (1995). Structure and function of voltage-gated ion channels. *Annual Review of Biochemistry* **64**, 493–531.

Cavalie, A., Ochi, R., Pelzer, D. & Trautwein, W. (1983). Elementary currents through Ca^{2+} channels in guinea pig myocytes. *Pflügers Archiv* **398**, 284–297.

Chad, J. E. & Eckert, R. (1985). An enzymatic mechanism for Ca^{2+} current inactivation in dialysed *Helix* neurons. *Journal of Physiology* **378**, 31–51.

Costantin, J. L., Qin, N., Waxham, M. N., Birnbaumer, L. & Stefani, E. (1999). Complete reversal of run-down in rabbit cardiac Ca^{2+} channels by patch-cramming in *Xenopus* oocytes; partial reversal by protein kinase A. *Pflügers Archiv* **437**, 888–894.

Deisseroth, K., Bito, H. & Tsien, R. W. (1996). Signaling from synapse to nucleus: postsynaptic CREB phosphorylation during multiple forms of hippocampal synaptic plasticity. *Neuron* **16**, 89–101.

Deisseroth, K., Heist, E. K. & Tsien, R. W. (1998). Translocation of calmodulin to the nucleus supports CREB phosphorylation in hippocampal neurons. *Nature* **392**, 198–202.

De Jongh, K. S., Murphy, B. J., Colvin, A. A., Hell, J. W., Takahashi, M. & Catterall, W. A. (1996). Specific phosphorylation of a site in the full-length form of the α_1 subunit of the cardiac L-type Ca^{2+} channel by adenosine 3′,5′-cyclic monophosphate-dependent protein kinase. *Biochemistry* **35**, 10392–10402.

Fabiato, A. & Fabiato, F. (1979). Ca^{2+} and cardiac excitation-contraction coupling. *Annual Review of Physiology* **41**, 473–484.

Gao, T., Yatani, A., Dell'Acqua, M. L., Sako, H., Green, S. A., Dascal, N., Scott, J. D. & Hosey, M. M. (1997). cAMP-dependent regulation of cardiac L-type Ca^{2+} channels requires membrane targeting of PKA and phosphorylation of channel subunits. *Neuron* **19**, 185–196.

Hagiwara, S. & Byerly, L. (1983). The Ca^{2+} channel. *Trends in Neurosciences* **6**, 189–193.

Hamill, O. P., Marty, A., Neher, E., Sakmann, B. & Sigworth, F. J. (1981). Improved patch clamp techniques for high resolution current recording from cells and cell free membrane patches. *Pflügers Archiv* **391**, 85–100.

Hao, L.-Y., Kameyama, A. & Kameyama, M. (1999). A cytoplasmic factor, calpastatin and ATP together reverse run-down of Ca^{2+} channel activity in guinea-pig heart. *Journal of Physiology* **514**, 687–699.

Hao, L.-Y., Kameyama, A., Kuroki, S., Nishimura, S. & Kameyama, M. (1998). Run-down of L-type Ca^{2+} channels occurs on the α_1 subunit. *Biochemical and Biophysical Research Communications* **247**, 844–850.

Hivert, B., Luvisetto, S., Navangione, A., Tottene, A. & Pietrobon, D. (1999). Anomalous L-type Ca^{2+} channels of rat spinal motoneurones. *Journal of General Physiology* **113**, 679–693.

Höfer, G. F., Hohentanner, K., Baumgartner, W., Groschner, K., Klugbauer, N., Hofmann, F. & Romanin, C. (1997). Intracellular Ca^{2+} inactivates L-type Ca^{2+} channels with a Hill coefficient of ∼1 and an inhibition constant of ∼4 μM by reducing channel's open probability. *Biophysical Journal* **73**, 1857–1865.

Hofmann, F., Biel, M. & Flockerzi, V. (1994). Molecular basis for Ca^{2+} channel diversity. *Annual Review of Neuroscience* **17**, 399–418.

Josephson, I. R. & Varadi, G. (1996). The beta subunit increases Ca^{2+} currents and gating charge movements of human cardiac L-type Ca^{2+} channels. *Biophysical Journal* **70**, 1285–1292.

Kameyama, A., Hao, L.-Y., Takano, E. & Kameyama, M. (1998). Characterization and partial purification of the cytoplasmic factor that maintains cardiac Ca^{2+} channel activity. *Pflügers Archiv* **435**, 338–343.

Kameyama, A., Yazawa, K., Kaibara, M., Onzo, K. & Kameyama, M. (1997). Run-down of the cardiac Ca^{2+} channel: Characterization and restoration of channel activity by cytoplasmic factors. *Pflügers Archiv* **433**, 547–556.

Kameyama, M., Kameyama, A., Nakayama, T. & Kaibara, M. (1988). Tissue extract recovers cardiac Ca^{2+} channels from 'run-down'. *Pflügers Archiv* **412**, 328–330.

Kameyama, M., Kameyama, A., Takano, E. & Maki, M. (1998). Run-down of the cardiac L-type Ca^{2+} channel: partial restoration of channel activity in cell-free patches by calpastatin. *Pflügers Archiv* **435**, 344–349.

Kavalali, E. T., Hwang, K. S. & Plummer, M. R. (1997). cAMP-dependent enhancement of dihydropyridine-sensitive Ca^{2+} channel availability in hippocampal neurons. *Journal of Neuroscience* **17**, 5334–5348.

Kepplinger, K. J. F., Kahr, H., Förstner, G., Sonnleitner, M., Schindler, H., Schmidt, T., Groschner, K., Soldatov, N. M. & Romanin, C. (2000). A sequence in the carboxy-terminus of the α_{1C} subunit important for targeting, conductance and open probability of L-type Ca^{2+} channels. *FEBS Letters* **477**, 161–169.

Klöckner, U., Mikala, G., Varadi, M., Varadi, G. & Schwartz, A. (1995). Involvement of the carboxyl-terminal region of the α_1 subunit in voltage-dependent inactivation of cardiac Ca^{2+} channels. *Journal of Biological Chemistry* **270**, 17306–17310.

Kostyuk, P. G. (1984). Intracellular perfusion of nerve cells and its effects on membrane currents. *Physiological Reviews* **64**, 435–454.

Lorca, T., Galas, S., Fesquet, D., Devault, A., Cavadore, J. C. & Doree, M. (1991). Degradation of the proto-oncogene product p39mos is not necessary for cyclin proteolysis and exit from meiotic metaphase: requirement for a Ca^{2+}-calmodulin dependent event. *EMBO Journal* **10**, 2087–2093.

McDonald, T. F., Pelzer, S., Trautwein, W. & Pelzer, D. (1994). Regulation and modulation of Ca^{2+} channels in cardiac, skeletal and smooth muscle cells. *Physiological Reviews* **74**, 365–507.

Molinari, M. & Carafoli, E. (1997). Calpain: A cytosolic proteinase active at the membranes. *Journal of Membrane Biology* **156**, 1–8.

Murphy, T. H., Worley, P. F. & Barbaran, J. M. (1991). L-type voltage-sensitive Ca^{2+} channels mediate synaptic activation of immediate early genes. *Neuron* **7**, 625–635.

Neher, E. (1992). Correction for liquid junction potential in patch clamp experiments. *Methods in Enzymology* **207**, 123–131.

Ono, K. & Fozzard, H. A. (1992). Phosphorylation restores activity of L-type Ca^{2+} channels after rundown in inside-out patches from rabbit cardiac cells. *Journal of Physiology* **454**, 673–688.

Peterson, B. Z., DeMaria, C. D. & Yue, D. T (1999). Calmodulin is the Ca^{2+} sensor for Ca^{2+}-dependent inactivation of L-type Ca^{2+} channels. *Neuron* **22**, 549–558.

Quin, N., Olcese, R., Bransby, M., Lin, T. & Birnbaumer, L. (1999). Ca^{2+}-induced inhibition of the cardiac Ca^{2+} channel depends on calmodulin. *Proceedings of the National Academy of Sciences of the USA* **96**, 2435–2438.

Rios, E. & Brum, G. (1987). Involvement of dihydropyridine receptors in excitation-contraction coupling in skeletal muscle. *Nature* **325**, 717–720.

Romanin, C., Grösswagen, P. & Schindler, H. (1991). Calpastatin and nucleotides stabilize cardiac Ca^{2+} channel activity in excised patches. *Pflügers Archiv* **418**, 86–92.

Schmid, R., Seydl, K., Baumgartner, W., Groschner, K. & Romanin, C. (1995). Trypsin increases availability and open probability of cardiac L-type Ca^{2+} channels without affecting inactivation induced by Ca^{2+}. *Biophysical Journal* **69**, 1847–1857.

Schultz, D., Mikala, G., Yatani, A., Engle, D. B., Iles, D. E., Segers, B., Sinke, R. J., Weghuis, D. O., Klockner, U. & Wakamori, M. (1993). Cloning, chromosomal localization, and functional expression of the α_1 subunit of the L-type voltage-dependent Ca^{2+} channel from normal human heart. *Proceedings of the National Academy of Sciences of the USA* **90**, 6228–6232.

Seydl, K., Karlsson, J. O., Dominik, A., Gruber, H. & Romanin, C. (1995). Action of calpastatin in prevention of cardiac L-type Ca^{2+} channel run down cannot be mimicked by synthetic calpain inhibitors. *Pflügers Archiv* **429**, 503–510.

Sheng, M., McFadden, G. & Greenberg, M. E. (1990). Membrane depolarization and Ca^{2+} induce c-fos transcription via phosphorylation of transcription factor CREB. *Neuron* **4**, 571–582.

Spaetgens, R. L. & Zamponi, G. W. (1999). Multiple structural domains contribute to voltage-dependent inactivation of rat brain α_{1E} Ca^{2+} channels. *Journal of Biological Chemistry* **274**, 22428–22436.

Soldatov, N. M. (1992). Molecular diversity of L-type Ca^{2+} channel transcripts in human fibroblasts. *Proceedings of the National Academy of Sciences of the USA* **89**, 4628–4632.

Soldatov, N. M. (1994). Genomic structure of human L-type Ca^{2+} channel. *Genomics* **22**, 77–87.

Soldatov, N. M., Oz, M., O'Brien, K. A., Abernethy, D. R. & Morad, M. (1998). Molecular determinants of L-type Ca^{2+} channel inactivation. *Journal of Biological Chemistry* **273**, 957–963.

Soldatov, N. M., Zühlke, R. D., Bouron, A. & Reuter, H. (1997). Molecular structures involved in L-type Ca^{2+} channel inactivation. *Journal of Biological Chemistry* **272**, 3560–3566.

Towbin, H., Staehelin, T. & Gordon, L. (1979). Electrophoretic transfer of proteins from polyacrylamide gels to nitrocellulose sheets: procedure and some applications. *Proceedings of the National Academy of Sciences of the USA* **76**, 4350–4354.

Wei, X., Neely, A., Lacerda, A. E., Olcese, R., Stefani, E., Perez-Reyes, E. & Birnbaumer, L. (1994). Modification of Ca^{2+} channel activity by deletions at the carboxyl terminus of the cardiac α_1 subunit. *Journal of Biological Chemistry* **269**, 1635–1640.

Yazawa, K., Kameyama, A., Yasui, K., Li, J.-M. & Kameyama, M. (1997). ATP regulates cardiac Ca^{2+} channel activity via a mechanism independent of protein phosphorylation. *Pflügers Archiv* **433**, 557–562.

Yokota, H., Katayama, M., Hino, F., Kato, I., Takano, E., Maki, M., Hatanaka, M. & Murachi, T. (1991). Direct measurement of calpastatin subtypes by sandwich enzyme immunoassay using monoclonal antibodies. *Molecular and Cellular Probes* **5**, 261–269.

Zühlke, R. D., Pitt, G. S., Deisseroth, K., Tsien, R. W. & Reuter, H. (1999). Calmodulin supports both inactivation and facilitation of L-type Ca^{2+} channels. *Nature* **399**, 159–162.

Acknowledgements

We thank N. Klugbauer, F. Hofmann (Munich) and V. Flockerzi (Heidelberg) for the gifts of clones of β_{2a} and $\alpha_2\delta$ subunits. This work was supported by the Austrian Science Foundation P12803 to T.S., P12728 to C.R., SFB Biomembranes F715 and P12667 to K.G., NB 7000 to C.R. and AHA to N.M.S. We wish to thank Badia AlBanna, Sabine Buchegger, Ingrid Gegenleitner and Bettina Kenda for their excellent technical assistance.

Corresponding author

C. Romanin: Institute for Biophysics, University of Linz, Altenbergerstrasse 69, A-4040 Linz, Austria.

Email: christoph.romanin@jk.uni-linz.ac.at